

# Computational Modeling of Electromechanical Behaviors of Dielectric Elastomer Actuators

Woosang JUNG, Yutaka TOI

**Abstract**— This paper presents a computational system which describes a electromechanical behaviors of dielectric elastomer actuators. In order to consider the large deformations, hyperelastic models such as the Mooney-Rivlin and Yeoh model are tested. Furthermore, time-dependent mechanical behaviors of dielectric elastomers are simulated by using 4<sup>th</sup>-order Prony series. The material parameters of visco-hyperelastic models are determined from experimental results. In particular, the influence of the first and second strain invariants for the Mooney-Rivlin model has been investigated to determine the material parameters reasonably. The mechanical and electromechanical behaviors of dielectric elastomers under various loading conditions have been simulated by using ANSYS considering thickness dependence of the dielectric constant. The predictions of the Mooney-Rivlin model for overall actuations show a good agreement with the experimental data and the validity of the present model has been demonstrated.

**Index Terms**— Computational Mechanics, Finite Element Method, Dielectric Elastomer Actuators, Electromechanical Analysis

## I. INTRODUCTION

In recent years, novel actuators using electroactive polymers (EAPs) have been developed in various fields such as MEMS, bio-mimetic robot and artificial muscles. EAP actuators transform electrical energy directly into mechanical work and produce large strain and stress [1]-[3].

Generally, there are two classes of electroactive polymers, ionic EAPs and electronic EAPs [1]. Actuations of ionic EAPs such as conducting polymers (CPs) and ionic conducting polymer-metal composites (IPMCs) are driven by diffusion of ions. They can be operated at a low driven voltage of 1~3V and actuated under wet conditions. However, there is a need to maintain wet condition and their response speed is slow. In contrast, electronic EAPs have advantages such as rapid response speed and relatively large actuation forces even though their actuations are driven by a high volt- age of several kilovolts.

Among the various EAP materials, dielectric elastomer, which belong to the electronic EAPs, have been investigated

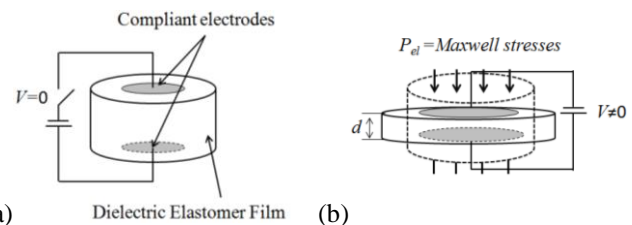


Fig.1 Structure and schematic diagram of actuation of dielectric elastomer: (a) voltage off and (b) voltage on

as intelligent materials due to their outstanding features such as large strain, high energy density, lightweight and high speed of response [2]-[12]. Dielectric elastomer actuators consist of a thin elastomer film with two compliant electrodes as shown in Fig.1.

When a differential voltage is applied to compliant electrodes, electrostatic force, which is so called “Maxwell stress”, are generated in the elastomer film. Then, the elastomer film contracts in the thickness direction and expands in the in-plane directions due to material incompressibility. According to the Perline’s equation [4], the electrostatic pressure acting on the insulating elastomer film can be calculated from a given applied voltage and film thickness as described in Eq.(1).  $\epsilon_0$  is the vacuum permittivity and  $\epsilon_r$  is the dielectric constant:

$$P_{el} = \epsilon_0 \epsilon_r \left( \frac{V}{d} \right)^2 \quad (1)$$

In order to simulate the electromechanical behaviors of dielectric elastomer actuators, a large number of constitutive equations have been proposed. G. Kofod [9]-[10] has investigated the dielectric property of the elastomer and tested a few hyperelastic models to describe uniaxial behaviors under isotonic and isometric conditions. The results of the Ogden model match well with experimental data. P. Lochmatter [11] proposed a quasi-static electromechanical modeling of the planer dielectric elastomer actuators with a hyperelastic film model. N. Goulbourne [12] presented the mathematical model of electromechanical response of fiber reinforced dielectric elastomers. On the other hand, M. Wissler [5-8] proposed various visco-hyperelastic models for circular dielectric elastomer actuators and performed lots of experiments for the validation of the proposed models. Among the various hyperelastic models, the results of the Yeoh model match well with experimental data under a certain pre-strain condition but show the large discrepancies under different pre-strain levels.

In most of the studies which have been conducted by

Manuscript submitted December 7, 2009.

Woosang JUNG is with the Institute of Industrial Science, University of Tokyo, 4-6-1 Komaba, Meguro-ku, Tokyo 153-8505, Japan. (Corresponding author: TEL +81-3-5452-6179, FAX +81-3-5452-6646, E-mail : [wjung@iis.u-tokyo.ac.jp](mailto:wjung@iis.u-tokyo.ac.jp)).

Yutaka TOI is with the Institute of Industrial Science, University of Tokyo, 4-6-1 Komaba, Meguro-ku, Tokyo 153-8505, Japan. (E-mail : [toi@iis.u-tokyo.ac.jp](mailto:toi@iis.u-tokyo.ac.jp)).

various hyperelastic models such as the Yeoh, Arruda-Boyce and Ogden model, the predictions for uniaxial behaviors of dielectric elastomer actuators show a good agreement with the experimental results. However, these models are not sufficient to predict the electromechanical behaviors of circular dielectric elastomer actuators under a multi-axial loading condition. One of the reasons for this is that the proposed hyperelastic models in the former researches consider mainly the influence of the first strain invariant and the second strain invariant is neglected.

The purpose of the present study is to develop the computational system which predicts the electromechanical behaviors of dielectric elastomer actuators under various loading conditions and applied voltages. For considering the influence of the second strain invariant, the Mooney-Rivlin model is used. The material parameters of the Mooney-Rivlin model have been determined from the identification procedures based on physical experiments including relaxation test, tensile test and circular actuation test. Then, finite element analysis has been conducted by using a general-purpose software ANSYS. The calculated results are compared with the experimental data

This article is organized as follows. Constitutive equations are presented in Sec.2. In Sec. 3, identification procedures of the material parameters are given. In Sec.4, finite element analysis is conducted and the results are compared with experimental data. Finally, concluding remarks and future works are given in Sec.5.

## II. CONSTITUTIVE MODEL

### A. Hyperelastic model

In order to describe the large deformations of dielectric elastomer actuators, hyperelastic material models are generally used. In particular, the constitutive behaviors of hyperelastic materials are usually derived from the strain energy potentials with the assumption that the hyperelastic material like rubber and elastomer is isotropic and nearly incompressible. For a incompressible material, the Cauchy stress,  $t_i$ , can be expressed as:

$$t_i = \lambda_i \frac{\partial W}{\partial \lambda_i} - p \quad (2)$$

where

$$\lambda_i = \frac{l}{l^0} = 1 + \varepsilon_i \quad (3)$$

$l$  is the current length and  $l^0$  is the original length.  $p$  is the hydrostatic pressure.  $\lambda_i$  and  $\varepsilon_i$  are the principle stretch ratio and the engineering strain in  $i$ th direction, respectively. The strain energy potential  $W$  can be a direction function of the stretch ratios or strain invariants as described in Eq.(4).  $I_1$  and  $I_2$  are the first and second strain invariants, respectively. The third invariant is constant ( $I_3=1$ ) due to material incompressibility:

$$W = W(I_1, I_2) \quad \text{or} \quad W = W(\lambda_1, \lambda_2, \lambda_3) \quad (4)$$

where

$$\begin{aligned} I_1 &= \lambda_1^2 + \lambda_2^2 + \lambda_3^2 \\ I_2 &= \lambda_1^{-2} + \lambda_2^{-2} + \lambda_3^{-2} \end{aligned} \quad (5)$$

There are several forms of strain energy potentials. As previously mentioned, the Mooney-Rivlin model is used to consider the influence of the second strain invariant. The strain energy potential of the Mooney-Rivlin model is expressed as follows:

$$W = C_{10}(I_1 - 3) + C_{01}(I_2 - 3) \quad (6)$$

Substituting Eq.(6) into (2), the Cauchy stress can be rewritten in tensor form :

$$\mathbf{t} = 2C_{10}\mathbf{B} + 2C_{01}\mathbf{B}^{-1} - p\mathbf{I} \quad (7)$$

where  $\mathbf{I}$  is the identity matrix.  $\mathbf{B}$  is the Finger tensor which can be defined from the deformation gradient tensor  $\mathbf{F}$  as described in Eq.(8).

$$\mathbf{F} = \begin{bmatrix} \lambda_1 & 0 & 0 \\ 0 & \lambda_2 & 0 \\ 0 & 0 & \lambda_3 \end{bmatrix}, \quad \mathbf{B} = \mathbf{F} \cdot \mathbf{F}^T = \begin{bmatrix} \lambda_1^2 & 0 & 0 \\ 0 & \lambda_2^2 & 0 \\ 0 & 0 & \lambda_3^2 \end{bmatrix} \quad (8)$$

In order to evaluate the validity of the Mooney-Rivlin model, the Yeoh model is also considered in this study. The strain energy potential of the Yeoh model is the function of the first strain invariant without considering the second strain invariant. The Cauchy stress for the incompressible Yeoh model is expressed as follows:

$$\mathbf{t} = 2 \frac{\partial W}{\partial I_1} \mathbf{B} - p\mathbf{I} \quad (9)$$

where

$$\frac{\partial W}{\partial I_1} = \sum_i^N i C_i (I_1 - 3)^{i-1} \quad (10)$$

### B. Viscoelastic model

The time-dependent mechanical response of dielectric elastomers can be described by using a quasi-linear viscoelastic model (QLV model [13]). In the QLV model, the material parameters in the strain energy potential are dependent on time but independent of the deformation. The time dependency of material parameters can be expressed by using 4th-order Prony series expansion of the dimensionless relaxation modulus as shown in Eq.(11):

$$C_{ij}^R = C_{ij}^0 \left( 1 - \sum_{i=1}^4 g_i \left( 1 - e^{-t/\tau_i} \right) \right) = C_{ij}^0 f(t) \quad (11)$$

$C_{ij}^0$  is the instantaneous elastic response and  $C_{ij}^R$  is relaxed elastic response.  $g_i$  and  $\tau_i$  are material parameters which characterize the relaxation behavior.

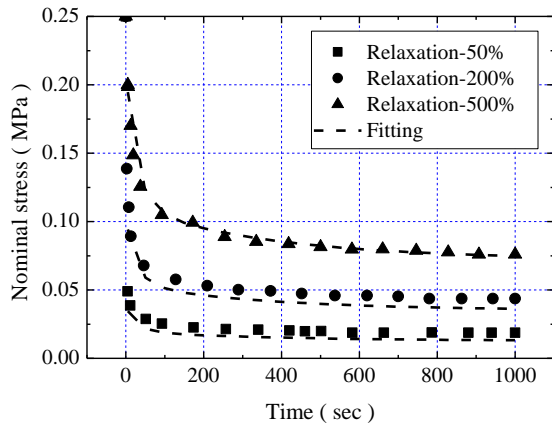


Fig.2 Stress relaxation tests when nominal strains of 50%, 200% and 500% are applied to the elastomer film: the filled symbols and the dash line represent the experimental data and curve fitting, respectively.

The above material parameters of the visco and hyperelastic models can be determined from experiment data obtained by uniaxial tensile test, stress relaxation test and circular actuation test. The details for evaluation of material parameters are presented in the following section.

### III. IDENTIFICATION OF MATERIAL PARAMETERS

According to the work given by M. Wissler [6], the Mooney-Rivlin model is not appropriate to describe the hyperelastic behaviors of dielectric elastomers. The predicted voltages by the Mooney-Rilvin model are about four times larger than experimental data. These discrepancies result from identification procedures which consider only uniaxial behaviors of dielectric elastomers. In this study, the material parameters are determined by the following three steps. In particular, the biaxial behaviors of dielectric elastomers are characterized by  $C_{01}$  of the Mooney-Rivlin mode in Step.3.

- i) Material parameters of the Prony-series are determined from relaxation tests
- ii)  $C_{10}$  of the Mooney-Rivlin model is determined from uniaxial tensile test.
- iii)  $C_{01}$  of the Mooney-Rivlin model is determined from circular actuator test under  $\lambda_p = 5, 3KV$

It is notable that  $C_{10}$  and  $C_{01}$ , the material parameters of the Mooney-Rivlin model, are evaluated separately and the reason for this will be discussed.

#### A. Material parameters of the viscoelastic model

Based on relaxation tests shown in Fig.2, the material parameters of the viscoelastic model are determined. The length/width ratio of each sample for relaxation tests is 10.0 and its thickness is 1mm. For curve fitting, the following equation is used:

$$\sigma(t) = \sigma_{\infty} + \sum_{i=1}^4 \sigma_i \cdot \exp\left(-\frac{t}{\tau_i}\right) \quad (12)$$

$\sigma_{\infty}$ ,  $\sigma_i$  and  $\tau_i$  are determined from experimental data. As

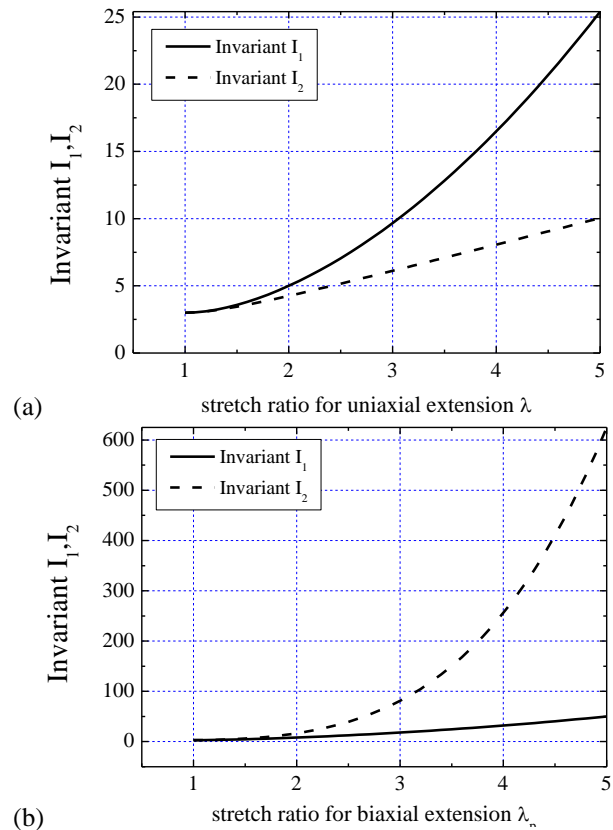


Fig.3 The first and second invariants under (a) uniaxial extension and (b) equi-biaxial extension

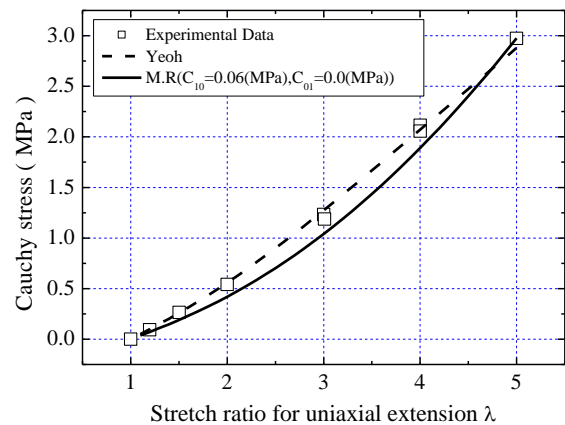


Fig.4 Uniaxial instantaneous hyperelastic responses: experimental data and the predictions of the Yeoh and Mooney-Rivlin model

previously mentioned, the relaxation function is independent of the deformations in QLV model. This means that the material parameters of the Prony series can be evaluated by coefficient comparison from  $\sigma_i$  and  $\tau_i$  as described in Eq. (13). The details for this process are given in Ref.[5].

$$\sum_{i=1}^4 \frac{\sigma_i}{\sigma_{\infty}} \cdot \exp\left(-\frac{t}{\tau_i}\right) = \frac{\sum_{i=1}^4 g_i \left(1 - e^{-t/\tau_i}\right)}{1 - \sum_{i=1}^4 g_i} \quad (13)$$

#### B. Material parameters of the Mooney-Rivlin model

Next, the material parameters of the Mooney-Rivlin model are evaluated. In order to determine the material parameters

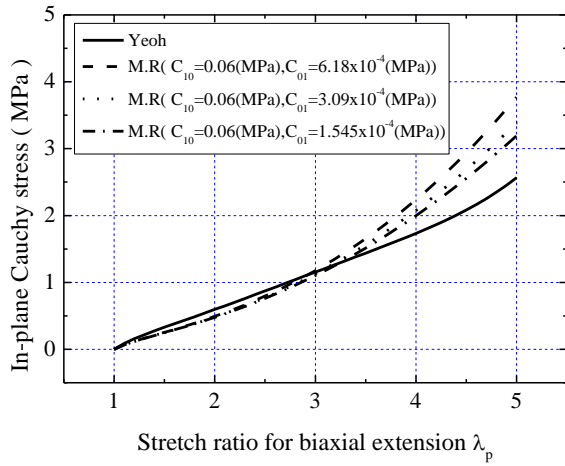


Fig.5 In-plane Cauchy stress under equi-biaxial extension and the responses with various  $C_{01}$

Table 1 Material parameters of the hyperelastic model

Mooney-Rivlin		Yeoh model[7]	
$C_{10}$	0.06(MPa)	$C_{10}$	0.0827(MPa)
$C_{01}$	$3.09 \times 10^{-4}$ (MPa)	$C_{20}$	$-7.47 \times 10^{-4}$ (MPa)
		$C_{30}$	$5.86 \times 10^{-6}$ (MPa)

Table 2 Material parameters of the viscoelastic model

Mooney-Rivlin		Yeoh model[7]	
$g_1$	0.57	$g_1$	0.478
$\tau_1$	0.311(s)	$\tau_1$	0.153(s)
$g_2$	0.189	$g_2$	0.205
$\tau_2$	3.35(s)	$\tau_2$	0.464(s)
$g_3$	0.086	$g_3$	0.0727
$\tau_3$	35.7(s)	$\tau_3$	32.021(s)
$g_4$	0.0543	$g_4$	0.0492
$\tau_4$	370(s)	$\tau_4$	215.85(s)

properly, the first and second strain invariants have been investigated and the calculated results are given in Fig.3. In the case of uniaxial extension, the increment of the first strain invariant at  $\lambda=5$  is about three times larger than that of the second strain invariant. On the other hand, the second strain invariant increases dramatically as an equi-biaxial extension ratio  $\lambda_p$  increases.

At first,  $C_{10}$  is determined from uniaxial extension test with the assumption that  $C_{01}$  is 0. The predicted Cauchy stresses of the Yeoh and Mooney-Rivlin models are in good agreement with experimental data (see Fig.4). The material parameters of the Yeoh model for this calculation are determined from optimization procedure presented by M. Wissler [7].

Unfortunately, no experimental data for the biaxial extension test are available in the literatures. In this study,  $C_{01}$  ( $=3.09 \times 10^{-4}$ ) is determined by comparisons between experimental and calculated results of circular actuators at  $\lambda_p=5$ , 3KV (will be discussed in Sec.4).

In Fig.5, the in-plane Cauchy stress under equi-biaxial extension has been investigated by using the coefficients obtained from the above procedures. As an equi-biaxial extension ratio  $\lambda_p$  increases, the predicted stress by the Moo-

Table 3 dielectric constant at different frequencies and pre-strain levels [8]

Pre-strain $\lambda_p$	$\epsilon_r$ at 100 Hz	$\epsilon_r$ at 10 kHz
1	$4.68 \pm 0.029$	$4.30 \pm 0.025$
3	$3.71 \pm 0.088$	$3.41 \pm 0.098$
4	$3.34 \pm 0.152$	$3.08 \pm 0.184$
5	$2.62 \pm 0.378$	$2.40 \pm 0.410$

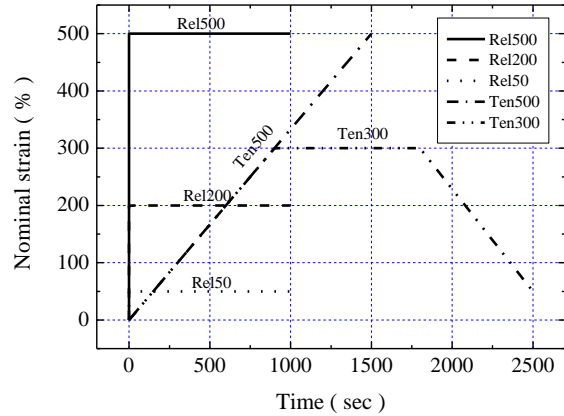


Fig.6 Input nominal strains vs. time for simulations of relaxation and tensile tests

ney-Rivlin model increases rapidly than the Yeoh model does. This means that the Mooney-Rivlin model presented in this study is appropriate to describe the effect of biaxial extension which can be significant at high strain. Although  $C_{01}$  is very small compared with  $C_{10}$ , the Fig.5 also shows that the Cauchy stress responses sensitively with increasing  $C_{01}$ . These results reveal that the predicted value of  $C_{01}$  is valid and the assumption ( $C_{01}=0.0$ ) used for the evaluation of  $C_{10}$  is reasonable. The material parameters for finite element analysis are given in table.1 and 2. The parameters of the Mooney-Rivlin model are determined from identification procedures (step.1~3) proposed in the present study and those of the Yeoh model are used in Ref.[7].

### C. Dielectric constant

The dielectric constant tends to decrease with decreasing thickness of elastomer. The value of dielectric constant which depends on the pre-strain ratio  $\lambda_p$  is given in Table 3 [8]. As the pre-strain ratio  $\lambda_p$  increases, the thickness and dielectric constant decreases. In the present study, dielectric constants at 100Hz are used for simulations by the Mooney-Rivlin model. In the case of the Yeoh model, the dielectric constant is assumed to be 4.7 and independent of pre-strain ratio [7].

## IV. FINITE ELEMENT ANALYSIS

### A. Simulations of uniaxial behaviors of dielectric elastomer film

In this section, the uniaxial behaviors of dielectric elastomer films are simulated. ANSYS has been used for the finite element analysis. The total number of eight-node hexahedron elements is 135 with 256 nodes [14]. The input strain profiles are given in Fig.6: relaxation tests (Rel50, Rel200, Rel500) and tensile tests (Ten300, Ten500). Fig.7 sh-

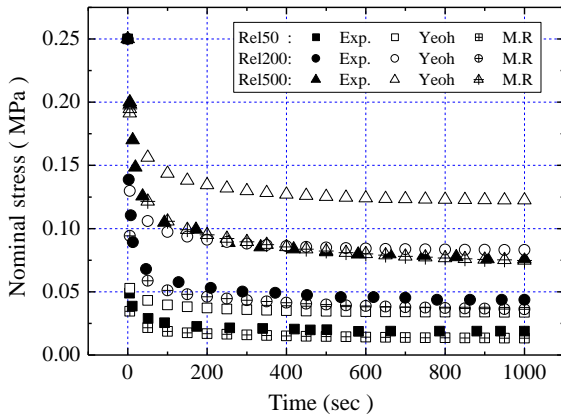


Fig.7 Relaxation tests: the experimental data and predicted nominal stress obtained by Yeoh and Mooney-Rivlin model.

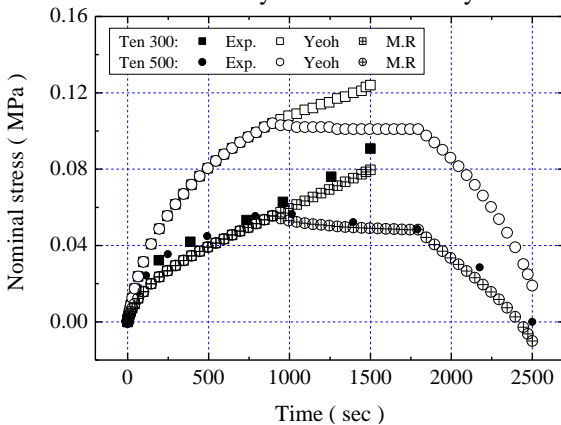


Fig.8 The experimental data and predicted nominal stresses corresponding to time history of tensile tests

ows the calculated results for relaxation tests. The results of the Yeoh model are not in good agreement with experimental data because the viscoelastic parameters of the Yeoh model are reoptimized to describe the behaviors of circular actuators (see Ref.[7]). On the other hand, the results of the present model (the Mooney-Rivlin model) show a good agreement with the experimental data because the viscoelastic material parameter is determined directly from relaxation tests. The simulated results for the tensile tests (Ten300, Ten500) are compared with experimental data in Fig.8. The calculated results by the Mooney-Rivlin model match well with experimental data, whereas the large discrepancy between experimental data and calculated results by the Yeoh model can be seen in Fig.8.

**B. Simulations of a pre-strained circular actuators under a applied voltage**

3-D deformation analysis with 8-node hexahedron elements has been conducted by using finite element model given in Fig.9. In general, circular actuators are pre-strained in order to improve their performance. The dielectric elastomer is extended in radial direction and fixed on a circular frame with radius  $R=75\text{mm}$ . Then, a circular area whose radius is  $7.5\text{mm}$  is coated with a mixture of graphite powder and silicone oil for electrodes. Its thickness is  $40\mu\text{m}$ . In the present study, the mechanical contribution of the electrode is neglected for simplicity.

The measured nominal radial strains under various pre-strain and voltage conditions are given in Fig.10. Under the assumption of material incompressibility, the reduction of

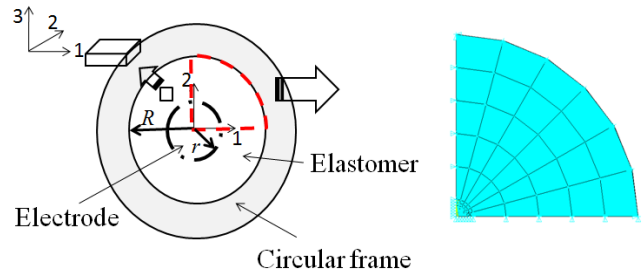


Fig.9 The circular actuator model

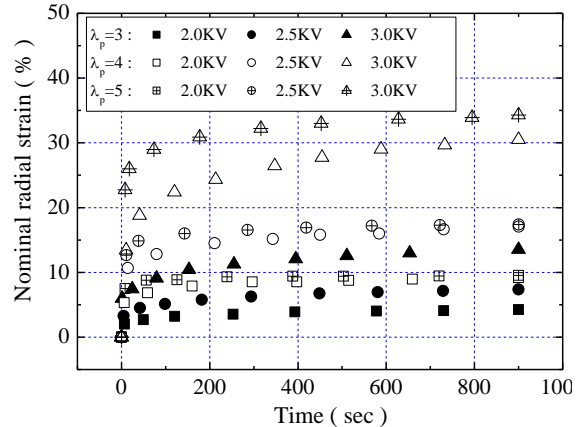


Fig.10 The nominal strain of pre-strained circular actuators under various voltages

thickness is calculated from time histories of the corresponding radial strains. Then, the thickness changes are used as a constrained condition for finite element analysis. The details for simulations are described as follows.

- i) Pre-strain  $\lambda_p$  in the radial direction is applied to a circular actuator.
- ii) Stress relaxation takes place for 1 hour
- iii) The stress  $t_3$  in thickness direction is obtained by using time history of thickness changes as a input data
- iv) The required voltage  $V$  is determined from the thickness and calculated compressive stress  $t_3$  :

$$P_{el} = \epsilon_0 \epsilon_r \left( \frac{V}{d} \right)^2 = -t_3 \tag{14}$$

Fig.11 shows the predicted voltages of the Yeoh model and Mooney-Rivlin models under a pre-strain ratio  $\lambda_p=3$ . The time histories of the calculated voltages obtained by the Yeoh and Mooney-Rivlin models show the same tendency. A large discrepancy during the initial reduction part of actuations means non-equilibrium in Eq.(14) because both Maxwell stress and compressive stress depend on the thickness of elastomer. The equilibrium state is satisfied as thickness changes comes to zero.

The time histories of the predicted voltages under a pre-strain ratio  $\lambda_p=4$  and 5 are given in Fig.12 and Fig.13, respectively. In Fig.14, the calculated results at the time 900 sec are summarized. The results of the Mooney-Rivlin model show the good approximations overall the pre-strain levels, whereas the large discrepancies between experimental data and the predicted voltages of the Yeoh model at pre-strain rat

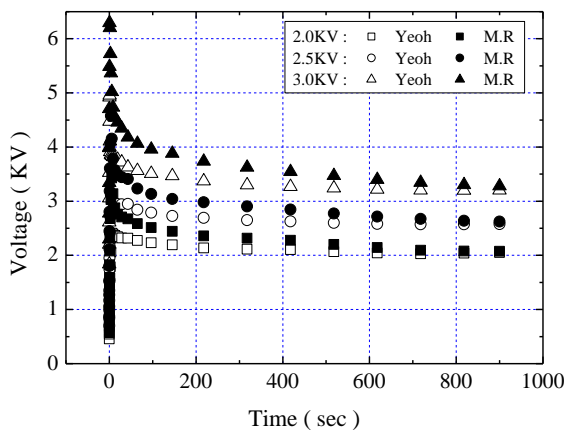


Fig.11 The predicted voltages under a pre-strain ratio  $\lambda_p=3$

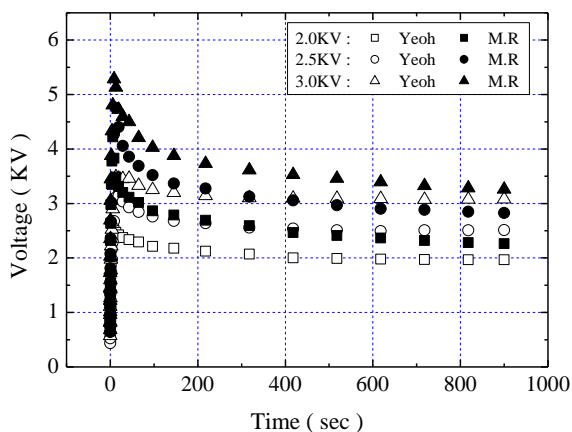


Fig.12 The predicted voltages under a pre-strain ratio  $\lambda_p=4$

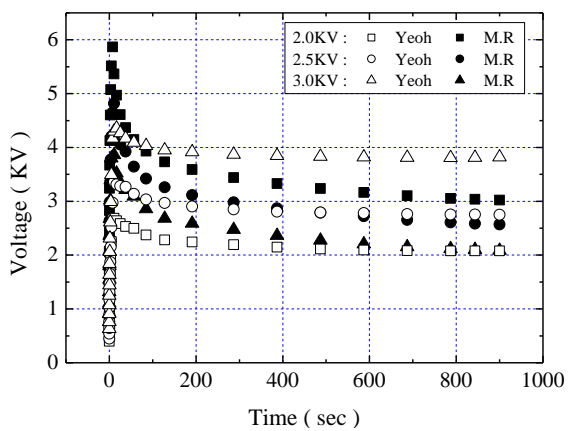


Fig.13 The predicted voltages under a pre-strain ratio  $\lambda_p=5$

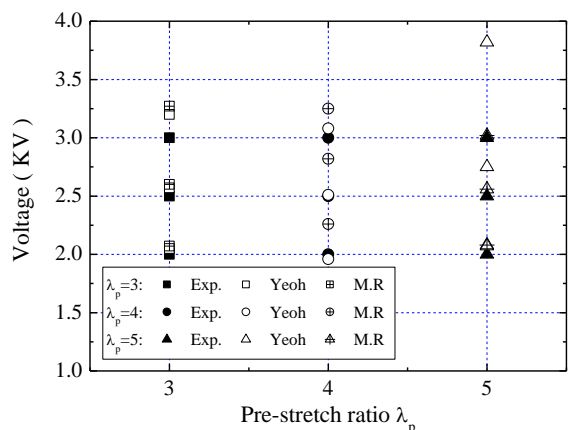


Fig.14 The experimental data and the predicted voltages of Yeoh-model and Mooney-Rivlin model at 900 sec

io  $\lambda_p=5$  can be seen in Fig.15.

## V. CONCLUSION

The aim of the present study is to develop the computational model for the electromechanical behaviors of dielectric elastomer actuators. In particular, the general validity of the present model over a wide range of stress and deformation states including uniaxial and multiaxial loading conditions has been investigated by using ANSYS.

The first and second strain invariants of the Mooney-Rivlin strain energy potential under uniaxial and equi-biaxial extension have been firstly investigated in order to determine material parameters properly. Then, the material parameters are determined from stress relaxation, tensile test and circular actuation test. The calculated results of the Mooney-Rivlin model show a good agreement with the experimental data and the validity of the present model has been demonstrated.

Although the proposed model can predict the electromechanical behaviors of dielectric elastomer actuators under various conditions, it also has some limitations. For example, thickness reduction of circular actuators is used as a constrained condition in the present study. However, to predict the deformations by using a voltage profile as an input condition is required in many applications. Future works are also focused on the improvement of the present model by the optimization of material parameters and investigation of higher order Mooney-Rivlin models.

## REFERENCES

- [1] Y. Bar-Cohen : "Electroactive polymer (EAP) actuators as artificial muscles – Reality, Potential and challenges", Vol. PM98, SPIE Press, Washington, (2001)
- [2] R.E. Pelrine, R. D. Kornbluh, Q. Pei, J. P. Joseph : "High-speed electrically actuated elastomers with strain greater than 100%", *Science*, 287, pp.836-39.(2000)
- [3] F. Carpi, D. De Rossi: "Dielectric elastomer cylindrical actuators: electromechanical modeling and experimental evaluation", *Materials Science & Engineering C*, Vol. 24, pp.555-62. (2004)
- [4] R.E. Pelrine, R. D. Kornbluh, J. P. Joseph : "Electrostriction of polymer dielectrics with compliant electrodes as a means of actuation", *Sensors and Actuators*, A 64, pp.77-85.(1998)
- [5] M. Wissler, E. Mazza: "Modeling and simulation of dielectric elastomer actuators", *Smart Materials & Structures*, Vol.14, pp. 1396-1402. (2005)
- [6] M. Wissler, E. Mazza: "Modeling and a pre-strained circular actuator made of dielectric elastomers", *Sensors and Actuators*, A 120, pp. 184-92. (2005)
- [7] M. Wissler, E. Mazza : "Mechanical behavior of an acrylic elastomer used in dielectric elastomer actuators", *Sensors and Actuators*, A 134, pp. 494-504. (2007)
- [8] M. Wissler, E. Mazza: "Electromechanical coupling in dielectric elastomer actuators", *Sensors and Actuators*, A 138, pp. 384-93. (2007)
- [9] G. Kofod : "Dielectric elastomer elastomers", Ph.D thesis, The Technical Univ. of Denmark, (2001)
- [10] G. Kofod and P. Sommer-Larsen: "Silicone dielectric elastomer actuators: Finite-elasticity model of actuation", *Sensors and Actuators*, A 122, pp. 273-83. (2005)
- [11] P. Lochmatter and G. Kovacs: "Design and characterization of an active hinge segment based on soft dielectric EAPs", *Sensors and Actuators*, A 141, pp. 577-87. (2008)
- [12] N. Goulbourne, E. Mockensturm and M. Frecker : "A nonlinear model for dielectric elastomer membranes", *Journal of Applied Mechanics*, Vol.72, pp.899-906. (2005)
- [13] Y.C. Fung : "Biomechanics : mechanical properties of living tissues", New York, 2<sup>nd</sup> edition, *Springer*, (1993)
- [14] Theory reference, ANSYS release 9.0, ANSYS, Inc.(2004)